J. A. Vásquez-Peralvo, J. C. Merlano-Duncán, Rakesh Palisetty, Vibhum Singh, Geoffrey Eappen, Jorge Luis González' - Ríos, S. Chatzinotas, "Wide-Beamwidth Circular Polarized Antenna for Diversity Combining applications," 2023 IEEE Global Communications Conference (GlobeCom), 2023.

Wide-Beamwidth Circular Polarized Antenna for Diversity Combining Applications

1st Juan A. Vásquez-Peralvo
Interdisciplinary Centre for Security, Reliability, and Trust (SnT)
Université du Luxembourg
Luxembourg, Luxembourg
orcid.org/0000-0001-7304-095X

2rd Juan Carlos Merlano Duncan
Interdisciplinary Centre for Security, Reliability, and Trust (SnT)
Université du Luxembourg
Luxembourg, Luxembourg
orcid.org/0000-0002-9652-679X

3rd Rakesh Palisetty
Interdisciplinary Centre for Security, Reliability, and Trust (SnT)
Université du Luxembourg
Luxembourg, Luxembourg
orcid.org/0000-0003-3222-6576

4th Vibhum Singh
Interdisciplinary Centre for Security, Reliability, and Trust (SnT)
Université du Luxembourg
Luxembourg, Luxembourg
orcid.org/0000-0003-4588-1924

5th Geoffrey Eappen
Interdisciplinary Centre for Security, Reliability, and Trust (SnT)
Université du Luxembourg
Luxembourg, Luxembourg
orcid.org/0000-0002-4065-3626

6nd Jorge Luis González-Rios
Interdisciplinary Centre for Security, Reliability, and Trust (SnT)
Université du Luxembourg
Luxembourg, Luxembourg
orcid.org/0000-0003-4415-9649

***Abstract*—This paper presents the design, simulation, and manufacturing of a right-hand circularly polarized antenna working in the frequency band 17.7-20.2 GHz with a beamwidth of 42.4° and 5.4° for the H-plane and E-plane, respectively. The presented antenna is part of a set of three antennas, two high-gain antennas, and, presented in this paper, a low directive antenna used for reception. The application we describe in this paper combines the radio-frequency signals obtained from the O3b satellite constellation, using three antennas to apply path diversity later to reconstruct the original signal. Moreover, using an antenna with a beamwidth in one plane allows receiving two satellite signals at the same time, increasing by 3 dB the overall gain. The wide-band capabilities of the antenna are obtained using aperture coupling. In particular, the circular polarization of the antenna is generated using a truncated corner square patch. Further, a metasurface is placed at the top to enhance the axial ratio. Importantly, the simulation results obtained using CST Microwave Studio show that the antenna has a reflection coefficient below -10 dB and an axial ratio below -3 dB in the intended frequency range.**

***Index Terms*—Antennas, circular polarization, metasurface, path diversity, wide beamwidth.**

I. Introduction

Satellite communications have evolved while providing access at any time and anywhere with an adequate line of sight. This satellite access has further enabled numerous multimedia applications with high data rates and more or less affordable costs [1]. Nevertheless, some of the applications are not economically feasible owing to the requirements of the user terminal. Therefore, there is an increasing research interest in user terminals for low Earth orbit (LEO), and medium Earth orbit (MEO) satellite orbits based on multi-link reception [2] and wide-beamwidth and low-gain antennas with a half-power beamwidth of 10° or bigger. The main idea is to combine multiple simultaneous satellite signals to improve the aggregated data rate and beam load balancing or enhance the satellite link's robustness through path diversity. Fig. 1 illustrates the main idea of the path diversity approach. The O3b satellite constellation consists of 15 active satellites located at the MEO satellite orbit with a revisit period of 6 hours [3]. Since all the satellites in this constellation have a similar period, inclination, apogee, perigee, and eccentricity, their orbital path will be almost the same. Therefore, from the user's point of view, there will be certain moments when multiple satellites are visible, describing the same orbit. Fig. 2 shows the elevation over a period of 6 hours of different O3b satellites visible from Luxembourg. Moreover, analyzing

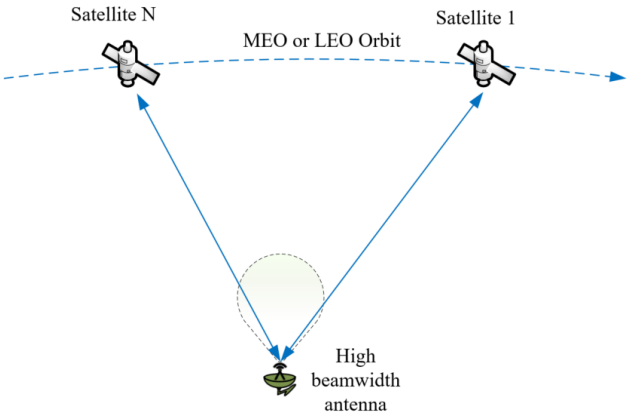

Fig. 1: Multi-satellite acquisition using a wide beamwidth antenna.

This work was supported by the Luxembourg National Research Fund (FNR), through the CORE Project (ARMMONY): Ground-based distributed beamforming harmonization for the integration of satellite and Terrestrial networks, under Grant FNR16352790, by the European Space Agency (ESA) under the project number 4000134678/21/UK/AL "User Terminal With Path Diversity For Constellations (DIVERSITY)," and SES S.A. (Opinions, interpretations, recommendations and conclusions presented in this paper are those of the authors and are not necessarily endorsed by FNR, ESA or SES).

J. A. Vásquez-Peralvo, J. C. Merlano-Duncán, Rakesh Palisetty, Vibhum Singh, Geoffrey Eappen, Jorge Luis González' - Ríos, S. Chatzinotas, "Wide-Beamwidth Circular Polarized Antenna for Diversity Combining applications," 2023 IEEE Global Communications Conference (GlobeCom), 2023.

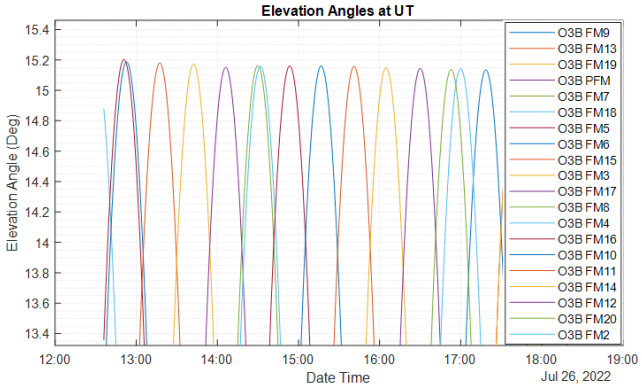

Fig. 2: Elevation angle vs time of O3b satellites visible from university of Luxembourg premises latitude = 49.626°, longitude = 6.159°.

the illustration, one can see that at certain times two satellites are visible at the same elevation angles. Thus, if we place a wide beamwidth antenna pointing to a specific azimuth and elevation angle, we can receive both signals.

In the literature, different types of solutions can be found for antenna design with high beamwidth in one plane and narrow in the other. For instance, sectoral, pillbox [4], lens [5], transmit [6], and reflect arrays [7] can be modeled to obtain a broader beamwidth in the H or E-plane while keeping the other narrow. However, some previous approaches have limitations in terms of bandwidth, manufacturing costs, and even inherent design in linear polarization. Some of the previously described limitations can be overcome using different techniques; for example, the intrinsic linear polarization of the antennas can be turned into a circular polarization by using frequency selective surface (FSS) polarizers [8] or orthomode transducers at the cost of overall manufacturing costs.

Motivated by the aforementioned discussion, this paper describes another approach using a metasurface-based antenna combined with an array of truncated square patch radiating elements. The square truncated patch antennas are fed by a distribution network with power dividers at the back of the antenna. The power dividers feed the antenna using aperture couplers, which have the inherent capabilities of increasing the antenna bandwidth. Importantly, the mentioned metasurface, which is located at the top of the antenna, enhances the circular polarization capabilities.

II. Antenna Design

We have set four stages to have an easy and effective antenna design process, as illustrated in Fig. 3. Each of the stages will be described separately.

A. Unit cell design

The antenna presented in this paper is partially based on the work presented in [9] and is composed of four layers, as illustrated in Fig. 4. Each layer has a RO4003C substrate, which has a permittivity of $\epsilon_r = 3.55$ and losses of $\tan\delta = 0.002$. In addition, the layers are joined using an FR4-based prepreg, which has a permittivity of $\epsilon_r = 3.8$ and losses of $\tan\delta = 0.002$.

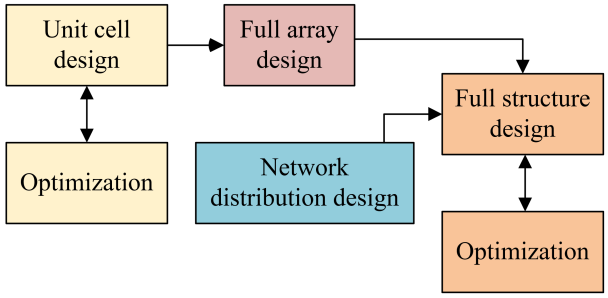

Fig. 3: Antenna design steps.

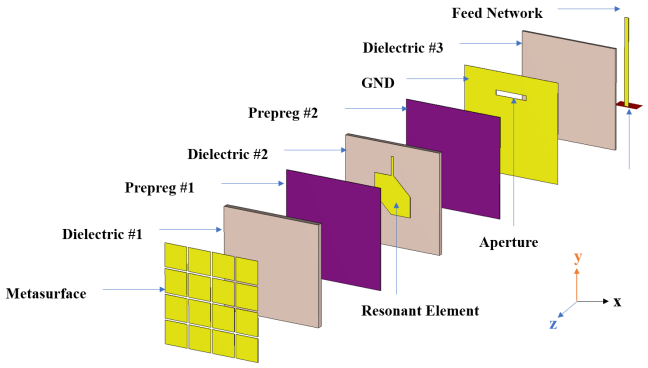

Fig. 4: Unit cell view layer by layer.

The unit cell design can be further analyzed in four stages.

a) Feed Network: The antenna is fed by a simple microstrip line with an impedance of 50 Ω. The length of the microstrip line extends around 0.65 mm over the top of the aperture. This extension reduces reflections acting as a stub.

b) Aperture: The primary purpose of the aperture is to feed the radiating element by induction of surface currents generated by the E-Field produced in the aperture due to the microstrip feed line. This feeding method has many advantages, for instance, shielding the antenna from spurious radiation, increasing bandwidth due to the contribution of the aperture radiation, and reducing manufacturing costs. Typically, the ratio between the aperture length a and width b is around 1/10 [10].

c) Radiating element: The right-hand circular polarization is achieved using a truncated corner square patch with dimensions qxq and truncation m. To improve the matching between the aperture and the truncated square patch, a short microstrip line of width d is extended from the middle to a length l.

d) Metasurface: The axial ratio of a printed antenna can be enhanced using a metasurface placed at the top [11]. For this reason, a 4×4 Sievenpiper structure has been placed on top of the truncated squared patch radiating element. The Sievenpiper structure has a gap g between elements, which

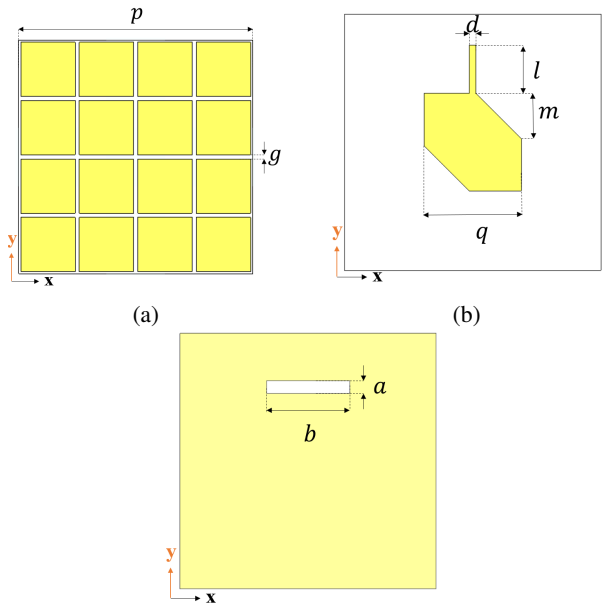

Fig. 5: Antenna dimensions (a) Metasurface; (b) Resonant element; (c) Aperture.

reduces or enhances the axial ratio.

To obtain the antenna dimensions that allow us to accomplish a reflection coefficient below -10 dB and an axial ratio below -3 dB, both in the bandwidth 17.7 - 20.2 GHz, an optimization process has been implemented using Thrust Region Framework. The antenna dimensions are presented in Fig. 5 where $p = 9.27$ mm, $g = 0.17$ mm, $d = 0.25$ mm, $l = 1.74$ mm, $q = 3.52$ mm, $m = 1.9$ mm, $a = 0.46$ mm, and $b = 3$ mm. The substrate thickness, starting from the bottom to top are $t_1 = 0.203$ mm, $t_2 = 0.406$ mm, and $t_3 = 0.508$ mm. Finally, the prepreg in all the layers that are used has a thickness of $t_4 = 0.05$ mm.

The unit cell has been simulated using CST Microwave Studio configured with the Frequency Domain Solver. The reflection coefficient and axial ratio are presented in Fig. 6, whereas, the realized gain in co-polar and cross-polar polarization are illuminated in Fig. 7. The simulation results show that the antenna addresses the required impedance bandwidth and axial ratio.

B. Array design

A good approximation to calculate the total number of elements can be obtained using the array factor (AF) formula in (1), where N is the total number of elements, k is the wavenumber, d is the inter-element spacing, and β is the progressive phase shift.

$$AF = \frac{\sin\left[N\frac{1}{2}\left(kd\cos\theta + \beta\right)\right]}{N\sin\left[\frac{1}{2}\left(kd\cos\theta + \beta\right)\right]}. \quad (1)$$

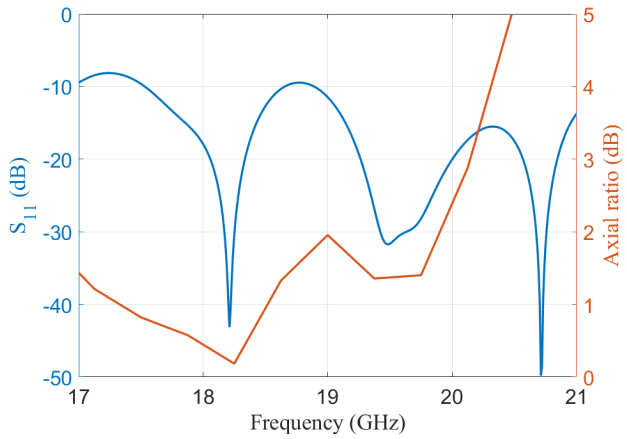

Fig. 6: Reflection coefficient and axial ratio in the frequency band of interest.

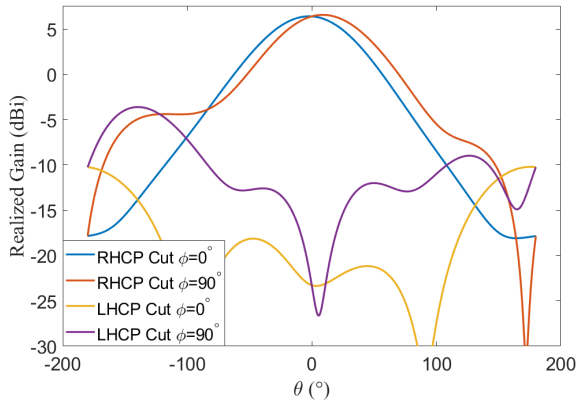

Fig. 7: Unit cell radiation pattern simulated at 19 GHz at different cuts for co and cross-polarization.

Now, considering the beamwidth as a design value while equating (1) to $\frac{1}{\sqrt{2}}$, and then simplifying, we obtain the total number of elements that can be approximated as

$$N \approx \frac{\text{asinc}\left(\frac{1}{\sqrt{2}}\right) 2\lambda_0}{\theta_{-3\text{dB}}\, d}. \quad (2)$$

where λ_0 is the free space wavelength, d is the inter-element spacing, and θ_{-3dB} is the desired beamwidth. Thus, using the design values given previously, we obtain that the array has two rows by sixteen columns, giving a total number of elements as $N = 32$.

C. Full structure design

The 32 antenna elements are now connected using a corporate feeding network consisting of interconnected power dividers terminated in the aperture coupling to the antenna. The microstrip lines are designed to reduce reflections significantly by using correct impedance matching, impedance transformers, cutting corners, and dents in junctions. Moreover, to reduce radiation pattern deformation due to connectors and

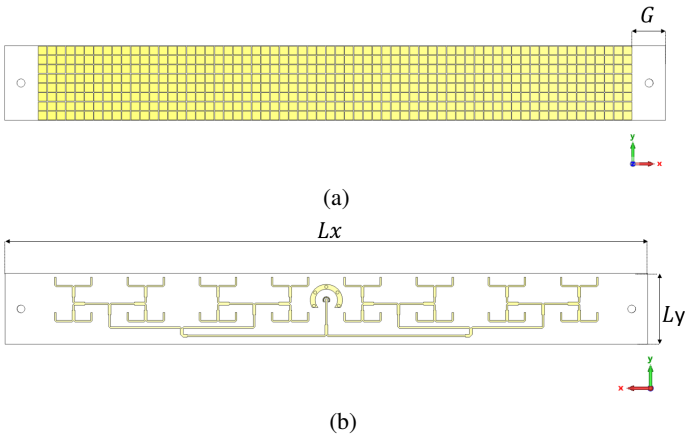

Fig. 8: Antenna array dimensions (a) Top view; (b) Bottom view.

cables coupling remarkably, the antenna is fed using a surface-mounted connector MMPX placed at the back of the antenna. Finally, the antenna is optimized to warrant a proper reflection coefficient and axial ratio. The dimensions of the final antenna are illustrated in Fig. 8.

The array antenna was simulated using a Time Domain Solver, considering a fine meshing in order to avoid miss leading results. The reflection coefficient and axial ratio simulations are illustrated in Fig. 9, whereas, the simulations related to the radiation pattern are depicted in Fig. 10 and Fig. 11. Analyzing the obtained results, one can see that the obtained reflection coefficient and axial ratio results address the initial requirements. In the case of the radiation pattern, the obtained beamwidth for the E-Plane and H-plane are around $\theta^{E}_{-3dB} = 42.4°$ and $\theta^{H}_{-3dB} = 5.4°$, respectively.

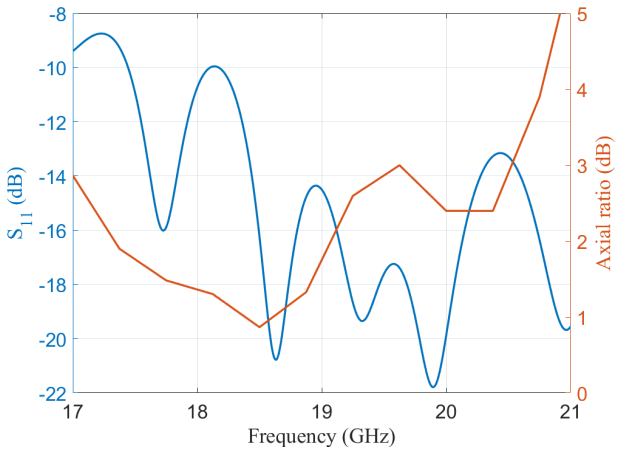

Fig. 9: Full array reflection coefficient and axial ratio in the frequency band of interest.

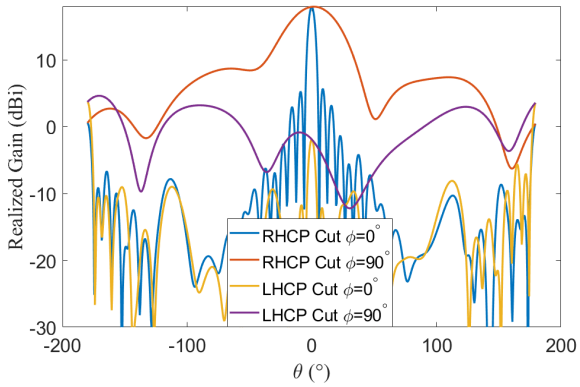

Fig. 10: Full array radiation pattern simulated at 19 GHz at different cuts for co-polarization and cross-polarization.

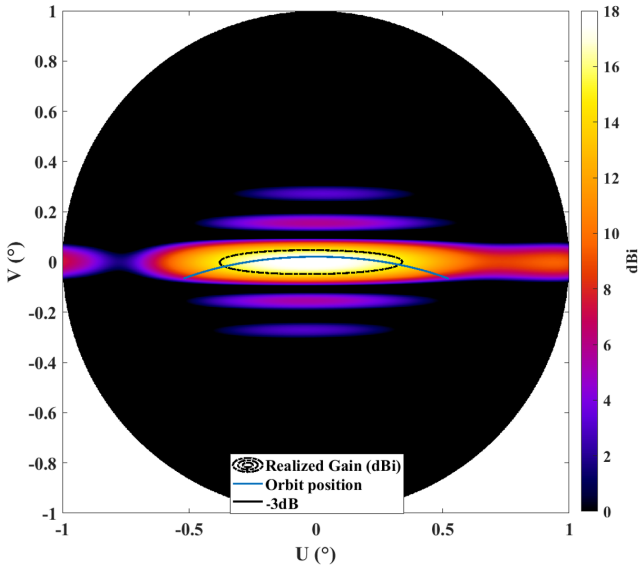

Fig. 11: Full array UV-plane Realized Gain simulated at 19 GHz. The figure also shows the -3dB contour offered by the antenna and the orbit described by the O3b constellation for a satellite passing over a ground station located at 49 Degrees Latitude.

III. Antenna Manufacturing

The antenna was manufactured using simple printing board circuit technology with the substrate and prepregs used for the design. In addition, two through holes have been included for measurement purposes, as illustrated in Fig. 12 (a). Moreover, since the connector MMPX is a surface-mounted connector, a proper grounding had to be designed. To improve the grounding, a set of multiple vias has been included to link the ground of the connectors to the antenna ground. Finally, the antenna measurements will be carried on using a compact test range and will be presented during the paper presentation.

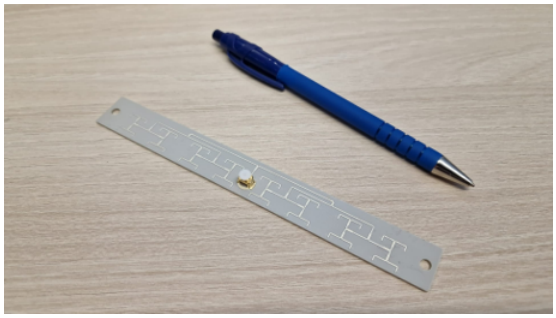

(a)

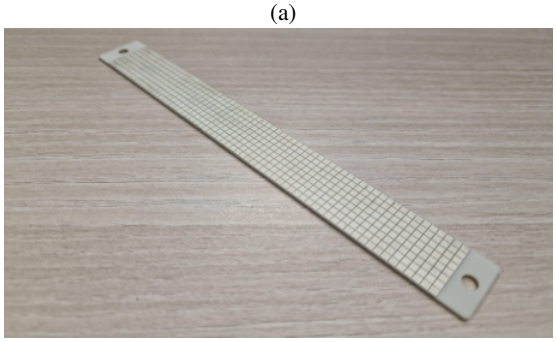

(b)

Fig. 12: Manufactured antenna array a) Top View. b) Bottom View

IV. ACKNOWLEDGMENT

The authors would like to acknowledge Société Européenne des Satellites for their support in this project.

V. CONCLUSIONS

Through this paper, we have presented the design, simulation, and manufacturing of a wide-beamwidth antenna used for diversity combining applications. The antenna beamwidth capabilities are obtained using 2×16 array elements of a circularly polarized patch antenna. We have demonstrated that by designing the antenna using aperture coupling for the cooperative distribution network and a metasurface at the top, a high bandwidth can be achieved with an AR below -3 dB.

REFERENCES

[1] P. Nannipieri, G. Dinelli, L. D. Sterpaio, A. Marino, and L. Fanucci, *Next-generation high-speed Satellite interconnect*. Springer, 2021.

[2] M.-A. Vázquez-Castro and N. Alagha, "Multi-link reception multibeam satellite system model," in *2012 6th Advanced Satellite Multimedia Systems Conference (ASMS) and 12th Signal Processing for Space Communications Workshop (SPSC)*, 2012, pp. 132–138.

[3] L. Wood, Y. Lou, and O. Olusola, "Revisiting Elliptical Satellite Orbits to Enhance the O3b Constellation," *Journal of the British Interplanetary Society*, vol. 67, pp. 110–118, Jan. 2014.

[4] S. Hay, J. Archer, G. Timms, and S. Smith, "A beam-scanning dual-polarized fan-beam antenna suitable for millimeter wavelengths," *IEEE Transactions on Antennas and Propagation*, vol. 53, no. 8, pp. 2516–2524, 2005.

[5] J. A. Vasquez-Peralvo, J. M. Fernandez-Gonzalez, and T. Wong, "3D Printed Discrete Dielectric Lens With Improved Matching Layers," in *2022 16th European Conference on Antennas and Propagation (EuCAP)*, 2022, pp. 1–5.

[6] P. Mei, S. Zhang, and G. F. Pedersen, "A low-profile and beam-steerable transmitarray antenna: Design, fabrication, and measurement [antenna applications corner]," *IEEE Antennas and Propagation Magazine*, vol. 63, no. 5, pp. 88–101, 2021.

[7] J. Yang, Y. Shen, L. Wang, H. Meng, W. Dou, and S. Hu, "2-D Scannable 40-GHz Folded Reflectarray Fed by SIW Slot Antenna in Single-Layered PCB," *IEEE Transactions on Microwave Theory and Techniques*, vol. 66, no. 6, pp. 3129–3135, 2018.

[8] H. L. Zhu, S. W. Cheung, K. L. Chung, and T. I. Yuk, "Linear-to-circular polarization conversion using metasurface," *IEEE Transactions on Antennas and Propagation*, vol. 61, no. 9, pp. 4615–4623, 2013.

[9] S. X. Ta and I. Park, "Low-profile broadband circularly polarized patch antenna using metasurface," *IEEE Transactions on Antennas and Propagation*, vol. 63, no. 12, pp. 5929–5934, 2015.

[10] D. Pozar, *Microwave Engineering Fourth Edition*, 2005.

[11] T. Nakamura and T. Fukusako, "Broadband design of circularly polarized microstrip patch antenna using artificial ground structure with rectangular unit cells," *IEEE Transactions on Antennas and Propagation*, vol. 59, no. 6, pp. 2103–2110, 2011.